

## Measuring the reabsorption cross section of a magneto-optical trap

Rudy Romain, H el ene Louis, Philippe Verkerk, and Daniel Hennequin\*

*Laboratoire PhLAM, CNRS UMR 8523, B atiment P5-Universit e Lille 1, 59655 Villeneuve d'Ascq Cedex, France*

(Received 27 February 2014; published 29 May 2014)

Magneto-optical traps have been used for several decades. Among fundamental mechanisms occurring in such traps, the magnitude of the multiple scattering is still unclear. Indeed, many experimental situations cannot be modeled easily, different models predict different values of the reabsorption cross section, and no simple experimental measurements of this cross section are available. We propose in this paper a simple measurement of this cross section through the size and the shape of the cloud of cold atoms. We apply this method to traps with a configuration where theoretical values are available and show that the measured values are compatible with some models. We also apply the method to configurations where models are not relevant and show that the reabsorption is sometimes much larger than the usually assumed value.

DOI: [10.1103/PhysRevA.89.053425](https://doi.org/10.1103/PhysRevA.89.053425)

PACS number(s): 37.10.Gh, 37.10.Vz, 42.25.Bs

### I. INTRODUCTION

The magneto-optical trap (MOT) is today an essential tool in experimental atomic physics. A MOT produces ultracold atoms which can be used in numerous experiments: MOTs are used, alone or with further cooling steps, to study quantum chaos [1], Anderson localization [2], and plasma instabilities [3,4]; to produce ultraprecise atomic clocks [5]; to obtain cold molecules [6]; and to carry out many other studies. In most cases, detailed knowledge of the cloud properties is not necessary. However, some studies focus on the MOT itself because it appears to be a potential model system for a wide class of physical problems, described by Vlasov-Fokker-Planck equations [4]. In this context, the study of the well-known instabilities experimentally observed in the MOTs is very interesting. These instabilities appear, for example, as a periodic motion of the center of mass of the cloud [7] or as an oscillation of the number of trapped atoms [7,8].

The study of these dynamics makes developing models much more elaborate than those describing only a single atom necessary. Indeed, it was shown that these instabilities are a collective behavior, and thus, models must take into account the interaction of each atom with all the other ones. Therefore, the only possible approach is to introduce macroscopic collective quantities, as in thermodynamics.

To introduce these quantities, let us remember that the cloud of cold atoms results from the interactions of the atoms with the laser light. The basic interaction is the absorption of a photon by an atom, followed by a spontaneous emission process. Depending in particular on the cloud density, the emitted photon can possibly undergo several cycles of absorption and emission before escaping the cloud: it is multiple scattering. The final cloud of cold atoms is the result of the equilibrium between the trapping force (induced by the exchange of momentum during the diffusion cycle), the shadow-effect force (induced by the absorption of the beam through the cloud), and the multiple-scattering force. As we are interested in the collective response of the cloud, we adopt a global formalism to take into account the interactions between all the atoms inside the cloud. Therefore, the amplitude of the forces will

be expressed in terms of cross sections:  $\sigma_L$  describes the absorption from the laser beams and  $\sigma_R$  is the reabsorption of scattered photons. Knowing these quantities is thus essential to model accurately a MOT, in particular the shape and dynamics of the resulting atomic cloud. Moreover, these cross sections play a key role in the analogy with plasma physics because the effective charge involved in the Coulomb-like interaction between cold atoms depends on their ratio [9].

These collective cross sections depend on the detailed mechanisms involved in a MOT, which are rather complex. Taking into account the exact distribution of the atomic levels and the interaction of the atoms with all the laser beams would lead to a very complex set of equations. As MOTs are operated with high laser intensity in the usual experimental configurations, it is not necessary to take into account sub-Doppler mechanisms. But even with such a simplification, the calculation of the cross sections requires some extra approximations. For example, although experimental MOTs are three-dimensional systems, most models consider a one-dimensional MOT in order to determine the atomic response inside the cloud, without taking into account the cross saturation, except in [10]. Thus, different models lead to different predictions. This is not a big deal concerning  $\sigma_L$  because simple absorption measurements lead to this quantity, and thus, it is easy to validate or invalidate a given model. On the contrary, no simple way to measure  $\sigma_R$  has been proposed until now. So theoretical predictions have never been validated by experimental measurements, and the  $\sigma_R$  values found today in the literature are still questionable.

We propose in this paper a method to measure the reabsorption cross section in a magneto-optical trap. We apply this method to a cesium trap and obtain values of  $\sigma_R$  for different sets of laser parameters. We compare these values to different models.

### II. THEORY

We consider here a MOT in the usual  $\sigma^+ - \sigma^-$  configuration. Each of the three arms of the trap consists of a pair of counter-propagating laser beams characterized by their intensity and their frequency. A pair is obtained by retroreflection of an incident beam. The beam intensities are  $I_+$  for the incident beam and  $I_-$  for the retroreflected one, while their frequency

\*daniel.hennequin@univ-lille1.fr

is given through the detuning  $\Delta$  between the laser frequency and the atomic transition.

As discussed above, we want here to describe the collective behavior of the atomic cloud. This requires two steps of calculation: the first one consists of describing the global behavior of the cloud through collective cross sections; the second one is the determination of the expressions of these cross sections. Only the second step requires us to detail the energetic structure of the cold atoms and could lead to different results following the degree of complexity chosen for the atomic structure. On the contrary, the relations established in the first step will be independent of this atomic structure.

Let us first establish the equations for the collective behavior of the atomic cloud. As discussed in the Introduction, the stationary cloud results from the equilibrium between three forces acting on the atoms. These forces have been expressed in numerous studies, with more or less approximations [4,9,11–13]. However, all these models deal with the same variables and the same parameters. The first force is the trapping force produced by the laser beams and the Zeeman shifts induced by the magnetic field. It is a restoring force, characterized by the spring constant  $\kappa$ . The two other forces are collective forces. The shadow-effect force is due to the absorption of the laser beams all along the cloud, leading to a local imbalance of the laser beam intensities. Thus, this force depends on the absorption cross section  $\sigma_L$ . Finally, the multiple-scattering force is induced by additional scattering of photons, and so it depends on the reabsorption cross section  $\sigma_R$ . The first two forces compress the cloud of atoms, while the latter causes it to expand. The size of the obtained atomic cloud is thus the result of an equilibrium between these three forces.

To study the equilibrium, we use an approach similar to that in [9] which assumes that the temperature of the cloud is zero. The main assumption in this model is that a photon is rescattered at most once before escaping the cloud. Contrary to [9], we consider the usual anti-Helmholtz configuration for the coils creating the magnetic field. Such a field is zero at the point defined as the center of the trap, and it can be assumed to be linear along each direction. We take into account the fact that the magnetic-field gradient along the coil axis is twice that along the perpendicular directions. So the spherical symmetry used in [9] is broken, and the cloud shape must be modeled as an ellipsoid.

The determination of the stationary density  $n$  does not require knowledge of the forces. Indeed, the collective forces depend on the shape of the cloud, while their divergences do not. The vanishing of the divergence of the total force (which is zero at equilibrium) gives us a constant atomic density. The results from [10], where a more general anisotropic configuration has been considered, can be applied to the present situation and give

$$n = \frac{2c\kappa}{3I_+ \sigma_L^2 (S - 1)}, \quad (1)$$

where  $S = \sigma_R/\sigma_L$  is the cross-section ratio and  $c$  is the speed of light. Note that as the quadrupolar magnetic field is taken into account, this expression differs slightly from that in [9,11].

We can improve this description of the MOT by calculating the expression of the three forces. The trapping force has

the usual form and takes into account the anisotropy of the magnetic-field gradient. The shadow-effect force has the same expression as is [9]; the absorption is assumed to be linear. The net multiple-scattering force is calculated as the sum over the cloud of all the Coulomb-like atom-atom interactions associated with a scattering process. Reference [10] shows how to calculate this force for an ellipsoidal cloud, with half widths  $L_{\parallel}$  and  $L_{\perp}$  along the coil axis and in the transverse plane, respectively. A geometric parameter  $A$ , depending only on the ellipticity  $\varepsilon = L_{\perp}/L_{\parallel}$  of the cloud, appears in the expression of the total force due to multiple scattering:

$$A = \frac{\varepsilon^2}{\varepsilon^2 - 1} \beta, \quad (2)$$

$$\beta = \begin{cases} 1 - \frac{1}{\sqrt{1-\varepsilon^2}} \ln \left| \frac{1+\sqrt{1-\varepsilon^2}}{1-\sqrt{1-\varepsilon^2}} \right| & \text{for } \varepsilon^2 > 1, \\ 1 - \frac{1}{\sqrt{\varepsilon^2-1}} \arcsin \left( \sqrt{\frac{\varepsilon^2-1}{\varepsilon^2}} \right) & \text{for } \varepsilon^2 < 1. \end{cases}$$

Note that this geometrical factor  $A$  does not depend on the total number of trapped atoms. Indeed, when the number of atoms varies, both widths change. But as the atomic density is constant, the ellipticity is conserved.

We have thus the expressions of the three forces along the coil axis. As we are interested in the steady state, the sum of the forces vanishes. The equilibrium of the forces gives another condition on this parameter:

$$A = \frac{1}{2} \left( 1 - \frac{1}{3S} \right). \quad (3)$$

Note that these relations are valid for both retroreflected and independent MOT configurations [10]. For the sake of completeness, let us mention that for a configuration with retroreflected beams, the equilibrium of the forces also gives us access to the cloud displacement due to the shadow effect. This displacement is global and depends only on the shadow effect: it gives no information about multiple scattering.

From the previous equations, it is easy to find that  $\varepsilon$  is bounded. First, the atomic density is a positive quantity so that, in Eq. (1),  $\sigma_R$  has to be larger than  $\sigma_L$  ( $S > 1$ ). It follows from Eq. (3) that  $A > 1/3$ . From the same equation, we also find that the maximum value of  $A$  is  $1/2$  (when  $S \rightarrow +\infty$ ). This leads to

$$1 < \varepsilon < 1.81. \quad (4)$$

Thus, the atomic cloud shape of the usual MOT appears to be always oblate. A spherical cloud corresponds to an infinite density and so is not a physical solution. We also point out an upper limit to the ellipticity which corresponds to  $\sigma_R \gg \sigma_L$ .

Figure 1 shows the cross-section ratio versus the ellipticity for all possible values: the more elongated the cloud is, the more probable the reabsorption is. This result is quite different from the one predicted for the temperature-limited regime in which the ellipticity of the cloud is constant and equal to  $\sqrt{2}$  [12]. In the multiple-scattering regime, the ratio  $S$  and the cloud ellipticity depend *a priori* on the laser parameters.

Now that we have characterized the cloud through the cross sections, we have to calculate them as a function of the laser parameters. As pointed out above, this calculation is rather complex. The atom must be modeled with a particular atomic structure from which the overlap between the emission

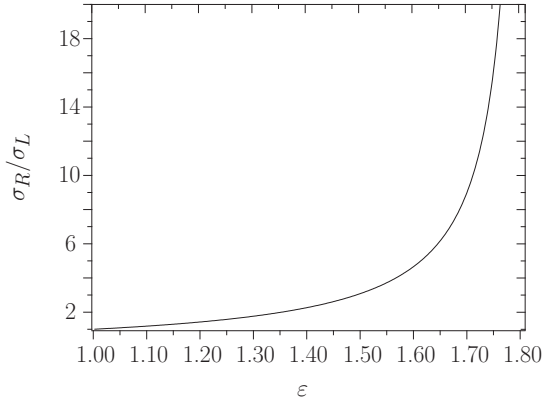


FIG. 1. Evolution of the cross-section ratio inside the predicted range of ellipticity values.

and the absorption spectra of a cold atom can be calculated. Several authors figured out theoretical expressions of  $\sigma_R$  in the context of Doppler cooling theory [4,9,11–13] but with different approaches. In [9], a fit of single cloud size measures is performed for only one set of parameter values. In [11] an approximated analytical calculation is done, while in [4,12,13] the dressed-atom picture (DAP) is used [14]. In all these studies, a two-level atom is considered, except in [4], which considers a three-level atom. These calculations take into account the saturation by the two counterpropagating beams, requiring us to introduce the total Rabi frequency  $\Omega = \Gamma\sqrt{(I_+ + I_-)/2I_{\text{sat}}}$ , with  $I_{\text{sat}}$  being the saturation intensity ( $I_{\text{sat}} = 1.1 \text{ mW/cm}^2$  for Cs) and  $\Gamma$  being the natural width of the transition.

Within the DAP, the secular approximation limits the range of parameter values to  $\Omega^2 + \Delta^2 \gg \Gamma^2$ . But even with such a simplification, the expression of  $\sigma_R$  remains heavy. Table I summarizes the expressions obtained by these previous studies in the two limit cases where the laser intensity is much larger than the detuning and vice versa. On the one hand, these two situations ( $|\Delta| \gg \Omega \gg \Gamma$  and  $\Omega \gg |\Delta| \gg \Gamma$ ) give simple asymptotic expressions. On the other hand, they represent the usual experimental parameters. Note that the values of parameters in [9] do not fit these two limit cases, and the results from [11] do not seem to be relevant. The expressions

TABLE I. Comparison of theoretical expressions for the cross-section ratio for the two limit cases,  $\Omega \gg |\Delta| \gg \Gamma$  and  $|\Delta| \gg \Omega \gg \Gamma$ .

Reference	$\Omega \gg  \Delta $	$\Omega \ll  \Delta $	Method
[11]	1	2	phenomenological calculation two-level atom
[12]	$\frac{\Delta^2}{2\Gamma^2}$	$\frac{3\Omega^2}{\Gamma^2}$	curve fitting DAP two-level atom
[13]	$\frac{\Delta^2}{3\Gamma^2}$	$\frac{\Omega^2}{2\Gamma^2}$	analytical expression DAP two-level atom
[4]	$\frac{\Delta^2}{6\Gamma^2}$	$\frac{\Omega^2}{2\Gamma^2}$	analytical expression DAP three-level atom

derived from the DAP give the same dependence on the laser parameters but with different numerical factors.

### III. MEASUREMENTS

Equations (2) and (3) link the cross-section ratio with the ellipticity. As ellipticity can be measured experimentally, we have a way to determine  $\sigma_R$  experimentally and to compare this measure to the theoretical predictions.

Our experimental setup is described in [7,15–17]: we use the usual MOT in which each arm is formed by the retroreflection of an incident beam. All incident beams have the same intensity. To guarantee repeatability and reproducibility of the measurements, special care was given to the technical parameters of the MOT in order to obtain homogeneous clouds. In particular, we used a single-mode optical fiber to clean the transverse profile of the beams. Moreover, we modulate the relative phases of all the beams to avoid possible interference patterns. The modulation frequency ( $>1 \text{ kHz}$ ) is chosen to be larger than the collective atomic response frequencies, so that the intensity is averaged. Finally, we carefully align the trap beams because the shape of the cloud is very sensitive to this alignment. Contrary to a MOT with six independent beams, our retroreflected configuration allows us to achieve accurate beam alignment (typically  $0.02 \text{ mrad}$ ).

In order to measure the ellipticity, we record the cloud fluorescence with a CCD camera, the optical axis of which is perpendicular to the coil axis. In that way, we obtain pictures showing a two-dimensional (2D) projection of the ellipsoid. The pictures are fitted on a 2D Gaussian, giving us the semiaxes  $L_{\parallel}$  and  $L_{\perp}$  of the ellipsoid. The exact relation between the fluorescence and the atomic density is not trivial. However, we are not interested in the density; we just want to compare the size of the cloud in both directions. A typical experimental measurement consists of recording the cloud sizes as a function of  $\Delta$  and repeating this sequence for different values of  $\Omega$ . For each set of parameters, we record ten pictures in order to improve the precision and to evaluate the standard deviation.

This method has a few limitations. It requires a good signal-to-noise ratio to monitor the cloud with a camera, which is not the case for dilute clouds, i.e., for large detunings or low laser intensities. On the other hand, in an asymmetric configuration

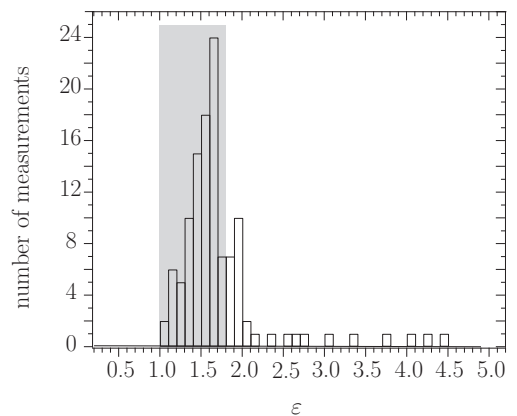


FIG. 2. Measures of the cloud ellipticity for 117 different values of the MOT parameters. The theoretical range is shown in gray.

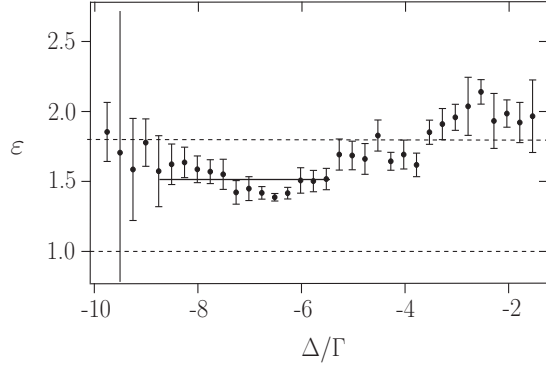


FIG. 3. Evolution of the ellipticity  $\varepsilon$  vs the laser detuning  $\Delta$  for  $I_+ \simeq 3.6I_{\text{sat}}$ . The dashed lines show the theoretical limits of ellipticity values ( $1 < \varepsilon < 1.81$ ). The error bars represent the standard deviation from the ten pictures.

such as the one used here, the shape of a thick cloud is degraded by the shadow effect. This occurs typically when the laser is tuned close to resonance. This issue does not exist for a MOT obtained with six independent beams. To sum up, we can expect in our case good-quality measures for intermediate detunings.

We first check the predicted range of ellipticity values. We measure the cloud sizes for almost 120 different values of  $(\Delta, \Omega)$ . Figure 2 shows all the measured values and how often they have been measured. The result is in rather good agreement with the theoretical range: about 90% (if we consider the error bars) of the measured ellipticities are inside the predicted range. No prolate cloud is observed.

Figure 3 shows the typical evolution of the ellipticity as a function of the detuning. In this example, the minimum value of the ellipticity is 1.4 and is measured around  $\Delta = -6.5\Gamma$ . We deliberately show here all the recorded points. However, let us remember that close to resonance, points are not relevant due to the shadow effect. We checked that all points with an ellipticity larger than 1.81 in Fig. 2 correspond to this situation. Thus, if we consider only points for which the method is valid, we find that all the measured ellipticities are smaller than the theoretical limit.

Strictly speaking, the two limit cases considered in Table I cannot be satisfied with our experimental parameter values. However, for large enough  $\Delta$  values, we approach the conditions  $|\Delta| \gg \Omega \gg \Gamma$ . Moreover, as the measurement quality is poor for very large detunings, we retain only

TABLE II. Comparison of the experimental determination of  $S$  with the predictions. For different intensity values, we give the average ellipticity  $\varepsilon$  measured for a range of large detunings, the deduced cross-section ratio  $S$ , and the theoretical value  $S_{\text{theor}}$  from [4,13].

$\Omega^2/\Gamma^2$	Detuning domain	$\varepsilon$	$S$	$S_{\text{theor}}$
4.5	$[-7.0\Gamma, -5.6\Gamma]$	$1.39 \pm 0.05$	$2.2^{+0.3}_{-0.3}$	2.3
7.0	$[-8.8\Gamma, -5.5\Gamma]$	$1.51 \pm 0.08$	$3.2^{+1.2}_{-0.7}$	3.1
9.4	$[-9.2\Gamma, -5.5\Gamma]$	$1.61 \pm 0.09$	$4.9^{+4.1}_{-1.6}$	4.7

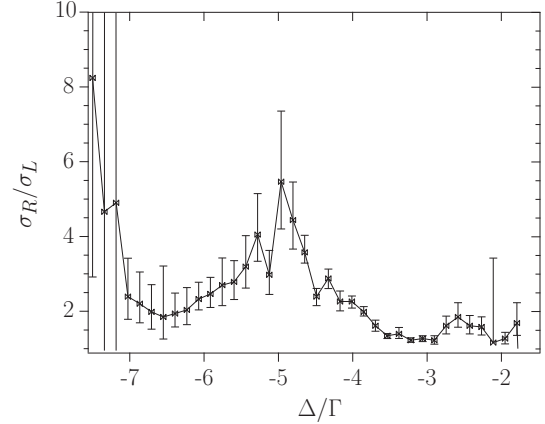


FIG. 4. Evolution of the cross-section ratio vs  $\Delta$  for  $I_+ \simeq 2.8I_{\text{sat}}$ .

intermediate values of the detuning for our determination of  $\varepsilon$ . This range matches the conditions where the method can be applied without restrictions. For example, in the case of Fig. 3, the estimation of the cross-section ratio is done in the range  $-8.8\Gamma < \Delta < -5.5\Gamma$ . In this case, we have  $\Omega \simeq \Gamma I_+/\sqrt{2}I_{\text{sat}} \simeq 2.5\Gamma$  and  $|\Delta| \gtrsim 2\Omega$ . Note that the secular limit is satisfied because  $\Omega^2 + \Delta^2 > 35\Gamma^2$ . In this interval, the ellipticity is quite constant, as predicted, and we get  $\varepsilon = 1.51 \pm 0.08$ , i.e.,  $\sigma_R = 3.2\sigma_L$ . This value is in good agreement with [4,13], which gives a theoretical value  $S_{\text{theor}}$  of 3.1.

Table II summarizes the measures obtained in three different configurations. In each case, the measure and the predicted value of  $S$  are very similar, with a relative difference of less than 5%. Unfortunately, despite the good precision on the ellipticity, the error on the cross section is significant. This is due to the nonlinearity of the relation between these two quantities (Fig. 1). Moreover, we get asymmetric errors because the derivative is also nonlinear. As a consequence the smaller the ellipticity is, the better the precision is.

Of course, the possibility to measure  $\sigma_R$  is particularly interesting for parameters where no theoretical predictions are available or where theoretical predictions are questionable because of the approximations. This is particularly the case for smaller detunings and intensities. Figure 4 shows the evolution of the cross-section ratio for  $-7.5\Gamma < \Delta < -1.8\Gamma$  and  $I_+ \simeq 2.8I_{\text{sat}}$ . It is interesting to note that  $S$  exhibits a maximum around  $\Delta = -5\Gamma$ , with values larger than 5. These values are rather high compared to those used in the literature, but they are consistent with Eq. (1). Close to the resonance, the ratio varies between 1 and 2, values which lead to a dense cloud, as expected for these detunings. However, far from resonance the ratio is a little bit larger than 2, but the density is small due to a weak restoring.

#### IV. CONCLUSION

In this paper, we propose a method to determine experimentally the reabsorption cross section  $\sigma_R$  in a cloud of cold atoms. This method allows us to measure  $\sigma_R$  for a large set of MOT parameter values. The method is nondestructive and is based on ellipticity measurements of the atomic cloud. The reabsorption cross section can be measured very easily. The

results of the measurements are in good agreement with the calculation done with the dressed-atom picture in the limit studied here (large detunings and intermediate intensities). We also make measurements for MOT parameters for which no theoretical predictions have been done. The measurements show that the cross-section ratio is underestimated in the literature in this case. We discuss the limitations of the method

regarding the MOT parameters and the trap configuration. The precision of this method can be as high as desired; it requires only more acquisitions. A good precision is needed especially when an important reabsorption is expected. Measuring the cross section can be very useful to improve our description of the reabsorption in future studies on spatiotemporal dynamics of the atomic cloud.

- 
- [1] S. Ghose, R. Stock, P. Jessen, R. Lal, and A. Silberfarb, *Phys. Rev. A* **78**, 042318 (2008).
- [2] F. Jendrzejewski, A. Bernard, K. Müller, P. Cheinet, V. Josse, M. Piraud, L. Pezzé, L. Sanchez-Palencia, A. Aspect, and P. Bouyer, *Nat. Phys.* **8**, 398 (2012).
- [3] H. Terças, J. T. Mendonça, and V. Guerra, *Phys. Rev. A* **86**, 053630 (2012).
- [4] R. Romain, D. Hennequin, and P. Verkerk, *Eur. Phys. J. D* **61**, 171 (2010).
- [5] N. Hinkley, J. A. Sherman, N. B. Phillips, M. Schioppa, N. D. Lemke, K. Beloy, M. Pizzocaro, C. W. Oates, and A. D. Ludlow, *Science* **341**, 1215 (2013).
- [6] *Cold Molecules: Theory, Experiment, Applications*, edited by R. Krems, B. Friedrich, and W. C. Stwalley (CRC Press, Boca Raton, FL, 2009).
- [7] A. di Stefano, P. Verkerk, and D. Hennequin, *Eur. Phys. J. D* **30**, 243 (2004).
- [8] G. Labeyrie, F. Michaud, and R. Kaiser, *Phys. Rev. Lett.* **96**, 023003 (2006).
- [9] D. W. Sesko, T. G. Walker, and C. Wieman, *J. Opt. Soc. Am. B* **8**, 946 (1991).
- [10] R. Romain, P. Verkerk, and D. Hennequin, *Eur. Phys. J. D* **67**, 211 (2013).
- [11] A. M. Steane, M. Chowdhury, and C. J. Foot, *J. Opt. Soc. Am. B* **9**, 2142 (1992).
- [12] C. G. Townsend, N. H. Edwards, C. J. Cooper, K. P. Zetie, C. J. Foot, A. M. Steane, P. Szriftgiser, H. Perrin, and J. Dalibard, *Phys. Rev. A* **52**, 1423 (1995).
- [13] L. Pruvost, I. Serre, H. T. Duong, and J. Jortner, *Phys. Rev. A* **61**, 053408 (2000).
- [14] C. Cohen-Tannoudji, J. Dupont-Roc, and G. Grynberg, *Atom-Photon Interactions* (Wiley, New York, 2004).
- [15] D. Wilkowski, J. Ringot, D. Hennequin, and J. C. Garreau, *Phys. Rev. Lett.* **85**, 1839 (2000).
- [16] A. di Stefano, M. Fauquembergue, P. Verkerk, and D. Hennequin, *Phys. Rev. A* **67**, 033404 (2003).
- [17] D. Hennequin, *Eur. Phys. J. D* **28**, 135 (2004).